

Requirements for estimating the volume of rocks and balls in a grinding mill

J. D. le Roux ^{*,1} I. K. Craig ^{*}

** Department of Electrical, Electronic and Computer Engineering,
University of Pretoria, Pretoria, South Africa.*

Abstract: This study aims to indicate which measurements are required in order to estimate the volume of rocks and balls in a semi-autogenous grinding mill as two separate states. The nonlinear observer model used here includes the following process states: water, solids, rocks, and balls in the mill, where solids are all ore small enough to discharge through the end-discharge grate, and rocks are all ore too large to discharge. The model includes the discharge rate, abrasion rate of rocks and the abrasion rate of balls as parameters. The available measurements are the total mill filling, the discharge flow-rate, and the discharge density. As seen from an observability analysis, the states and parameters become observable from the second-order time-derivatives of the measurements. The minimum set of measurements required for observability of all states and parameters is the mill filling, the discharge density, and the first and second-order time-derivatives of the discharge density. However, modelling the second-order time-derivative of the discharge density is problematic, as it assumes constant model parameters. Although the combined volume of rocks and balls can be estimated using measurements of the mill filling, the discharge flow-rate, the discharge density, and the first-order time-derivative of the discharge density, these measurements remain insufficient to distinguish between rocks and balls. To reliably distinguish between the rocks and balls in the mill, an additional measurement apart from the ones mentioned above is required. Since power draw models introduce large parameters sets of their own, another viable and reliable option is required.

Keywords: comminution, grinding mill, observability, parameter estimation, state estimation

1. INTRODUCTION

The main impediment to implementing model-based control in the mineral processing industry, and specifically grinding mills, is the lack of sufficient measurements to estimate the necessary states and parameters (Wei and Craig, 2009). The aim is to characterize plant operation from real-time measurements without the need for expensive and time-consuming sampling campaigns.

Considerable work has been done to estimate grinding mill process variables using different modelling approaches (Herbst et al., 1992). A very simple model along with power and bearing pressure measurements is used by Herbst et al. (1989) to estimate mill filling and rock hardness. This work was extended in Herbst and Pate (1996) to estimate ore, water, and ball inventories. A commercialised soft-sensor is described by Herbst and Pate (1999) to estimate mill inventories and breakage rates. In all cases a Kalman filter is used to estimate the unknown state vector. Although the filters capture the qualitative trend of the unknown state vector, the studies above do not explicitly include observability analyses to ensure the filters produce reliable solutions.

A linear observability test is included in the inferential measurement work of Apelt et al. (2002). The SAG mill model of Napier-Munn et al. (2005) was used to describe the grinding process, along with a novel ball charge model

and a mill-liner model. Using measurements of the mill charge weight and size-by-size solids discharge, Apelt et al. (2002) used 29 measurements to estimate 37 states and 7 parameters with an extended Kalman filter (EKF). However, the rank of the observability matrix of the linearised system was only 20, which meant a unique solution for the parameters and states was not available. In Olivier et al. (2012) and Le Roux et al. (2016a), the states are all observable such that a particle filter is capable of estimating the states. However, it is assumed that parameters such as ore hardness and ore size distribution remain constant.

In an attempt to address the issue of observability of grinding mill conditions, Le Roux et al. (2016c) developed a model for a semi-autogenous (SAG) grinding mill with states and parameters locally (weakly) nonlinearly observable. The states and parameters of the grinding mill model are:

- x_w - volume of water in the mill,
- x_s - volume of solids in the mill,
- x_r - volume of rocks in the mill,
- x_b - volume of balls in the mill,
- η - discharge rate of slurry from the mill,
- K_r - abrasion rate of rocks, and
- K_b - abrasion rate of balls.

The measurements used to estimate the states and parameters listed above are:

¹ Corresponding author. E-mail: derik.leroux@up.ac.za

- J_T - fraction of mill filled with charge,
- Q - slurry discharge flowrate, and
- ρ_Q - density of slurry discharge.

A nonlinear observer such as a moving horizon estimator (MHE) could potentially estimate the unknown states and parameters, but it is necessary to correctly assume the time-varying nature of the parameters for the MHE to estimate the true state and parameter values. A longer time horizon for the MHE reduces the validity of modelling the parameters as constants, but a shorter time horizon may not include sufficient system dynamics for the observer to estimate the unknown states and parameters.

As an alternative, an EKF could be considered to estimate the states and parameters. However, not all the states and parameters are observable for the linearised version of the model in Le Roux et al. (2016c). The rank of the observability matrix of the linearised system is 6, implying one of the states and parameters is not observable. Linear observability is desirable for the EKF since the states and parameters are estimated from a linearised version of the system at each time step.

It is not surprising that the linearised system's parameters and states are not observable considering neither the rocks (x_r) or balls (x_b) exit the mill. They are kept inside the mill by the discharge grate. Apart from the mill filling measurement J_T , where these states appear as a linear combination, no further information is available for these states. However, the observability analysis of the nonlinear system indicates that if sufficient dynamics are visible in the output, and a nonlinear observer is used, the individual contribution of the rocks and balls to J_T is distinguishable.

The model of Le Roux et al. (2016c) is reduced in Le Roux et al. (2016b) such that states and parameters are observable from the linearised version of the reduced model. The states and parameters for the reduced model are:

- x_w - volume of water in the mill
- x_s - volume of solids in the mill
- x_{rb} - volume of total grinding media
- η - discharge rate of slurry from the mill
- χ - accumulation rate of solids

The reduced model made use of the same measurements as the full model, but added the time-derivative of discharge density. Consequently, an EKF is applied in simulation to evaluate the effectiveness of the observer. Simulations indicate that with accurate mill discharge flow-rate, mill discharge density, and total mill charge measurements, it is possible to estimate the states and parameters of the reduced model. The main challenge is to accurately calculate the first-order time-derivative of the mill discharge density.

The disadvantage of the reduced model is that it lumps the rocks and balls together into one state. Ideally, it is necessary to estimate x_b independent of the rest of the charge. SAG mills are generally designed with a constant x_b in mind in order to produce a specific grind. Because accurate real-time measurements of x_b are not available, it remains a challenge to maintain a consistent x_b . Apelt et al. (2001) showed that x_b can be estimated using weight or powerdraw models, but the minimum uncertainty in the

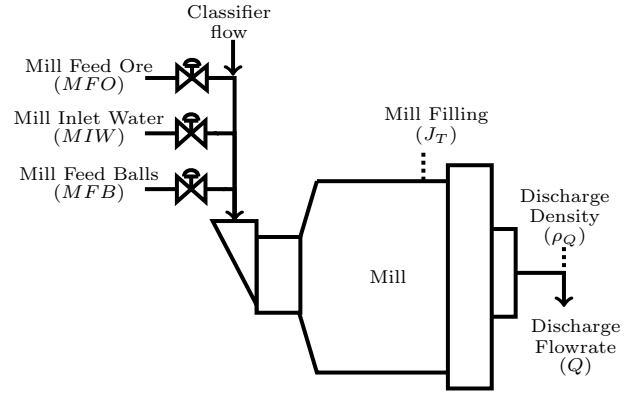


Fig. 1. A semi-autogenous grinding mill.

estimate is 25%. Generally a linear relationship between x_r and K_b is assumed, such that the feed rate of balls to the mill is set as a fraction of the feed rate of ore to the mill. Measurement of x_b will not only allow a controller to maintain a consistent x_b , but also to manipulate the grind by varying x_b .

Le Roux et al. (2016b) and Le Roux et al. (2016c) do not resolve what will be required for the states and parameters of the linearised version of the full nonlinear model to be fully observable. The aim of this work is to indicate what is required for all states and parameters of the full model to be observable, especially such that x_r and x_b can be uniquely distinguished.

Section 2 provides a description of the SAG milling process, and a brief overview of the nonlinear model of Le Roux et al. (2016c). Section 3 proceeds with a description of the requirements for observability of the linearised version of the nonlinear model. Conclusions are made in Section 4.

2. GRINDING MILLS

2.1 Process Description

The open circuit SAG mill depicted in Fig. 1 receives three streams: mined ore (MFO), water (MIW) and additional steel balls (MFB) to assist with the breakage of ore. If the mill circuit is closed with a classifier such as a hydrocyclone, the underflow from the hydrocyclone also flows into the mill. The mill charge constitutes a mixture of grinding media and slurry. Grinding media refers to the steel balls and large rocks used for breaking the ore, and slurry refers to the mixture of water and all ore material that exhibit the same flow characteristics as water. The fractional volumetric filling of the mill by the total charge is represented by J_T .

The mill is rotated along its longitudinal axis by a motor. As shown in Fig. 2, the charge in the mill is lifted by the inner liners on the walls of the mill to a certain height from where it cascades down, only to be lifted again by the rotating action of the mill. If the rotational speed is sufficiently fast, the material in the charge will become airborne after reaching the top of its travel on the mill shell. The uppermost point where material leaves the mill shell is defined as the shoulder of the charge. The airborne particles follow a parabolic path, reaching a maximum

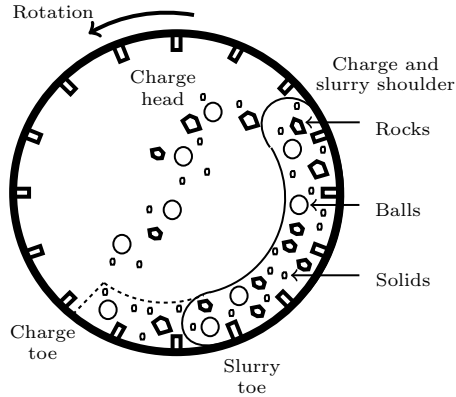


Fig. 2. Cross-section of a semi-autogenous grinding mill.

Table 1. Description of circuit variables.

Variable	Unit	Description
MIW	$[m^3/h]$	Flow-rate of water to the mill
MFO	$[t/h]$	Feed-rate of ore to the mill
MFB	$[t/h]$	Feed-rate of steel balls to the mill
J_T	$[-]$	Fraction of mill volume filled with charge
Q	$[m^3/h]$	Mill discharge flow-rate
ρ_Q	$[t/m^3]$	Mill discharge density

called the head and making contact again with the mill charge at the bottom of the mill. The cascading motion of the charge causes the ore to break through impact, abrasion and attrition. The mill grind is the fraction of material in the discharge of the mill below the specification size and indicates the efficiency of the mill to break the ore.

The ground ore in the mill mixes with the water to create a slurry. The slurry is discharged through an end-discharge grate where the aperture size of the end-discharge grate limits the particle size of the discharged slurry. The slurry in a mill begins to form at the shoulder of the charge. The toe of the slurry starts to grow downwards towards the toe of the charge with increasing flow-rate. While the toe of the slurry is less than or equal to the toe of the charge, discharge occurs via the grinding media. When the toe of the slurry exceeds the toe of the charge, a slurry pool forms at the bottom of the mill. Slurry discharge is then a combination of flow via the grinding media and the slurry pool. Slurry pool conditions should be avoided as it decreases the breakage rate by cushioning material falling from the charge shoulder to the charge toe (Latchireddi and Morrell, 2003). It is assumed that no slurry pooling occurs in the case where the discharge grate has a large open area of apertures, a high relative radial position of the open area, and a high relative radial position of the outermost apertures (Apelt et al., 2002). The flow-rate of slurry at the mill discharge is given by Q . It is assumed that the in-mill slurry density is equal to the discharge slurry density (ρ_Q). The variables assumed to be measured are listed in Table 1.

2.2 Model Description

A brief overview of the model in Le Roux et al. (2016c) is presented here. The nomenclature for the model can be seen in Table 2. The constituents in the mill are modelled as four volumetric quantities: water (x_w), solids (x_s), rocks (x_r), and balls (x_b). The model makes use of only two size

classes to describe ore in the mill: *solids* includes all ore smaller than the end-discharge grate aperture size, and *rocks* is all ore larger than the aperture size.

Process Dynamics The population balance used to describe the kinetics of the states defined above is

$$\dot{x}_w = V_{wi} - V_{wo} \quad (1a)$$

$$\dot{x}_s = V_{si} - V_{so} + RC \quad (1b)$$

$$\dot{x}_r = V_{ri} - RC \quad (1c)$$

$$\dot{x}_b = V_{bi} - BC \quad (1d)$$

where V_{wi} , V_{si} , V_{ri} , and V_{bi} are the mill inflow of water, solids, rocks, and balls respectively, V_{wo} and V_{so} (m^3/h) are the discharge of water and solids from the mill respectively, and RC and BC (m^3/h) are the consumption of rocks and balls respectively. Because the mill is fitted with an end-discharge grate, no rocks or balls are discharged from the mill. It is assumed the mill is a fully mixed reactor, and that discharge grate is such that no slurry pooling occurs.

The mill inflow flow-rates are

$$V_{wi} = MIW + V_{cw} \quad (2a)$$

$$V_{si} = MFO(1 - \alpha_r)/\rho_o + V_{cs} \quad (2b)$$

$$V_{ri} = \alpha_r MFO/\rho_o \quad (2c)$$

$$V_{bi} = MFB/\rho_b \quad (2d)$$

where ρ_o (t/m^3) is the density of the feed ore, ρ_b (t/m^3) is the density of the steel balls, and V_{cw} and V_{cs} (m^3/h) is the flow of water and solids returned by the classifier respectively. The parameter α_r defines the fraction of rock in MFO and is assumed to be measured as a function of time (Wei and Craig, 2009). It is assumed that the flow from the classifier to the mill is known.

Similar to the cumulative rates modelling approach (Hinde and Kalala, 2009), the consumption of rocks (RC) and balls (BC) in (1b) to (1d) are described as

$$RC = x_r K_r \quad (3a)$$

$$BC = x_b K_b \quad (3b)$$

where K_r and K_b ($1/h$) are the abrasion rates of rocks and balls respectively.

As shown in Morrell and Stephenson (1996), Q is quadratically proportional to the volume of slurry in the mill if there is no slurry pool. Thus, it is possible to express Q in terms of x_s and x_w as

$$Q = \eta (x_w + x_s)^2 \quad (4)$$

where $(x_w + x_s)$ represents the total slurry hold-up in the mill, and η ($h^{-1}m^{-3}$) is the discharge rate per volume of

Table 2. Nomenclature

Parm	Unit	Description
α_r	$[-]$	Fraction rock in the feed ore
ρ_b	$[t/m^3]$	Density of steel balls
ρ_o	$[t/m^3]$	Density of feed ore
ρ_w	$[t/m^3]$	Density of water
K_b	$[1/h]$	Ball abrasion factor
K_r	$[1/h]$	Rock abrasion factor
v_{mill}	$[m^3]$	Mill volume
η	$[h^{-1}m^{-3}]$	Discharge rate
x_w	$[m^3]$	Volume of water in the mill
x_s	$[m^3]$	Volume of solids in the mill
x_r	$[m^3]$	Volume of rocks in the mill
x_b	$[m^3]$	Volume of balls in the mill

slurry. Therefore, the discharge of the water (V_{wo}) and solids (V_{so}) in (1a) and (1b) can be expressed as

$$V_{wo} = \eta(x_w + x_s)x_w \quad (5a)$$

$$V_{so} = \eta(x_w + x_s)x_s. \quad (5b)$$

Process Measurements The assumed measurements are modelled as

$$J_T = \frac{x_w + x_s + x_r + x_b}{v_{mill}} \quad (6a)$$

$$Q = \eta(x_w + x_s)^2 \quad (6b)$$

$$\rho_Q = \frac{\rho_o x_s + \rho_w x_w}{x_s + x_w} \quad (6c)$$

The combined mass of the mill and of the charge inside the mill is generally measured using either load cells or bearing pressure (Wei and Craig, 2009). However, this is not a direct measurement of J_T , and a relation between J_T and the mass measurement needs to be determined. As shown by Powell et al. (2009, 2011), mill filling measurements during mill stops can be used to calibrate the relationship between the mass measurement and J_T . With careful planning, the mass to J_T relationship can easily be checked within half an hour from mill stop to start.

This study assumes measurements of Q and ρ_Q are available. Because of space restrictions at the discharge trommel of the mill, inclusion of flow and density instrumentation at the mill discharge is not yet a viable reality (Napier-Munn et al., 2005). Through careful planning and design of greenfield comminution circuits it should be possible to install existing flow and density instrumentation at a mill discharge trommel. In the case where the mill discharges into a sump, ρ_Q and Q can be back-calculated from a flow-balance if all inflows and outflows at the sump are measured, but this is highly sensitive to the accuracy of measurements at the sump. This study aims to illustrate the benefits to be gained from including Q and ρ_Q measurement instrumentation in industrial circuits.

3. OBSERVABILITY

A multi-input-multi-output control-affine non-linear state-space model with $\dim(x) = n$ and $\dim(y) = m$ can be written as

$$\begin{aligned} \dot{x} &= f(x) + g(x)u \\ y &= h(x). \end{aligned} \quad (7)$$

The system in (7) is said to be locally (weakly) observable at x_0 if there exists a neighbourhood X_0 of x_0 such that for every x_1 which is an element of the neighbourhood $X_1 \subset X_0$ of x_0 the indistinguishability of the states x_0 and x_1 implies that $x_0 = x_1$. The two states x_1 and x_0 are said to be indistinguishable if for every admissible input u the output y of (7) for the initial state x_0 and for the initial state x_1 is identical. If the system satisfies the so called observability rank condition, i.e. the observability codistribution of x_0 (Hermann and Krener, 1977)

$$d\mathcal{O} = \text{span} \left\{ dh_j, dL_f h_j, \dots, dL_f^{n-1} h_j \right\}; \quad j = 1, \dots, m \quad (8)$$

has dimension n at x_0 , then the system is locally (weakly) observable. Note, $L_f^k h_j$ refers to the k -th repeated Lie derivative of the scalar function $h_j(x)$ along the vector field $f(x)$, and d is the exterior derivative. In the linear case,

the observability codistribution corresponds to the observability matrix $\mathcal{O}^T = [C^T, A^T C^T, \dots, (A^{n-1})^T C^T]$ where $C = \frac{\partial h}{\partial x}|_{x=x_0}$ and $A = \frac{\partial}{\partial x}(f(x) + g(x)u)|_{x=x_0, u=u_0}$.

3.1 Nonlinear Observability

The observer model described in Section 2.2 can be written in the form of (7), such that

$$\dot{x} = \begin{bmatrix} -\eta(x_w + x_s)x_w \\ -\eta(x_w + x_s)x_s + x_r K_r \\ -x_r K_r \\ -x_b K_b \\ 0_{3 \times 1} \end{bmatrix} + \begin{bmatrix} I_{4 \times 4} \\ 0_{3 \times 4} \end{bmatrix} u \quad (9a)$$

$$y = \begin{bmatrix} \frac{x_w + x_s + x_r + x_b}{v_{mill}} \\ \eta(x_w + x_s)^2 \\ \frac{\rho_o x_s + \rho_w x_w}{x_s + x_w} \end{bmatrix} \quad (9b)$$

where $x = [x_w, x_s, x_r, x_b, \eta, K_r, K_b]^T$, $u = [V_{wi}, V_{si}, V_{ri}, V_{bi}]^T$, $y = [J_T, Q, \rho_Q]^T$, and parameters η , K_r and K_b are assumed to be unknown constants.

The repeated Lie derivatives of the system output with respect to the system dynamics are collected in a single vector, as shown below:

$$\begin{bmatrix} h \\ L_f h \\ L_f^2 h \end{bmatrix} = \begin{bmatrix} \frac{x_w + x_s + x_r + x_b}{v_{mill}} \\ \eta X_{ws}^2 \\ \frac{\rho_o x_s + \rho_w x_w}{X_{ws}} \\ -\frac{\eta X_{ws}^2 + K_b x_b}{X_{ws}} \\ -2\eta^2 X_{ws}^3 + 2\eta K_r x_r X_{ws} \\ \frac{x_w x_r K_r (\rho_o - \rho_w)}{X_{ws}^2} \\ \frac{2\eta^2 X_{ws}^3 - 2\eta K_r x_r (x_s + x_w) + K_b^2 x_b}{X_{ws}^2} \\ \frac{6\eta^3 X_{ws}^4 - 8\eta^2 K_r x_r X_{ws}^2 + 2\eta K_r^2 x_r X_{ws}}{X_{ws}^3} \\ \frac{x_w x_r K_r (\rho_o - \rho_w) (\eta X_{ws}^2 - 2K_r x_r - K_r X_{ws})}{X_{ws}^3} \end{bmatrix} \quad (10)$$

where $X_{ws} = x_w + x_s$.

Two observability codistributions are defined:

$$\begin{aligned} d\mathcal{O}_1 &= \text{span} \{ dh, dL_f h \} \\ d\mathcal{O}_2 &= \text{span} \left\{ dh, dL_f h, dL_f^2 h \right\}. \end{aligned}$$

The rank of $d\mathcal{O}_1$, which has 6 rows and 7 columns, is 6. This indicates that the addition of only the first order time-derivatives of the measurements are not sufficient for nonlinear observability. This is self-evident, as $d\mathcal{O}_1$ is row insufficient.

The rank of $d\mathcal{O}_2$, which has 9 rows and 7 columns, is 7. This indicates all system states are locally (weakly) observable from the available measurements. Since full rank is achieved for $d\mathcal{O}_2$, the addition of further Lie derivatives is not necessary. This indicates that second-order time-derivatives of the measurements are required for observability. This is comparable to the result of Le Roux and Craig (2016), where it is shown that second-order time-derivatives are required to algebraically calculate mill states and parameters.

3.2 Linear Observability

The states and parameters of the linearised version of the model in (9) is not observable (Le Roux et al.,

Table 3. Rank of observability matrix for different measurement sets.

Set	Measurements								Rank	
1	J_T	Q	ρ_Q	\dot{J}_T	\dot{Q}	$\dot{\rho}_Q$			6	
2	J_T	Q	ρ_Q	\dot{J}_T	\dot{Q}	$\dot{\rho}_Q$	\ddot{J}_T	\ddot{Q}	$\ddot{\rho}_Q$	7
3	J_T	Q	ρ_Q	\dot{J}_T	\dot{Q}	$\dot{\rho}_Q$	\ddot{J}_T			7
4	J_T	Q	ρ_Q	\dot{J}_T	\dot{Q}	$\dot{\rho}_Q$		\ddot{Q}		7
5	J_T	Q	ρ_Q	\dot{J}_T	\dot{Q}	$\dot{\rho}_Q$			$\ddot{\rho}_Q$	7
6	J_T	Q	ρ_Q	\dot{J}_T			\ddot{J}_T			6
7	J_T	Q	ρ_Q		\dot{Q}			\ddot{Q}		7
8	J_T	Q	ρ_Q			$\dot{\rho}_Q$			$\ddot{\rho}_Q$	7
9		Q	ρ_Q		\dot{Q}	$\dot{\rho}_Q$		\ddot{Q}	$\ddot{\rho}_Q$	5
10	J_T	Q		\dot{J}_T	\dot{Q}		\ddot{J}_T	\ddot{Q}		6
11	J_T	Q			\dot{Q}			\ddot{Q}		6
12	J_T		ρ_Q			$\dot{\rho}_Q$			$\ddot{\rho}_Q$	7
13		Q	ρ_Q			$\dot{\rho}_Q$			$\ddot{\rho}_Q$	5
14			ρ_Q			$\dot{\rho}_Q$			$\ddot{\rho}_Q$	5

2016c). However, from the discussion above, this can be altered if the second-order time-derivatives of the three measurements in (9) are included as measurements. The question now becomes which of the derivatives are essential, and which are superlative to achieve linear observability?

The measurements and their respective derivatives are shown in (11) below, where $V_{ws} = V_{wi} + V_{si}$. The rank of $\mathcal{O}^T = [C^T, A^T C^T, \dots, (A^{n-1})^T C^T]$ is evaluated to determine linear observability. Matrix $A = \frac{\partial}{\partial x} (f(x) + g(x)u)|_{x=x_0, u=u_0}$ is evaluated from (9a). Matrix $C = \frac{\partial h}{\partial x}|_{x=x_0}$ is evaluated using different combinations of the measurements listed in (11). These sets and the corresponding rank of \mathcal{O} is shown in Table 3. The combinations were chosen heuristically such that the contribution of each measurement and its second order derivative to the observability of \mathcal{O} is understood.

The 1st to 5th sets in Table 3 indicate that at least one second order derivative is required for all states to be estimated. The 6th set indicates that derivatives of J_T alone are insufficient to produce linear observability for all states. As seen from sets 7 and 8, if measurements of J_T , Q , and ρ_Q are available, derivatives of either Q or ρ_Q alone contain sufficient information for observability of all states. The 9th set indicates that J_T remains essential, even though its derivatives are not essential for observability of all states. The 10th and 11th sets indicate that ρ_Q is an essential measurement. As seen from set 12, J_T , ρ_Q , and the derivatives of ρ_Q are the bare minimum for linear observability. In the 13th set, only using Q , ρ_Q and the

derivatives of ρ_Q is not sufficient for full observability. The 14th set simply indicates that ρ_Q and its derivatives are not sufficient by themselves. Therefore, the critical measurements are J_T and ρ_Q .

The ability to distinguish between x_r and x_b from the measurements of J_T , Q , ρ_Q and the derivatives of ρ_Q is a desirable result. However, apart from the challenge to determine n -th order derivatives in the presence of significant measurement noise (Savitzky and Golay, 1964), another issue is of major concern. The model in (9a) assumes $\dot{\eta} = \dot{K}_r = \dot{K}_b = 0$, which is a simplifying assumption as the time-varying nature of these parameters are unknown. When the time-derivatives of the outputs in (9b) are taken, the assumption of constant parameters influence the expression of the derivatives. For example, Q is a function of η . If the derivative of Q is taken, the derivative of η should be taken into consideration such that the symbolic representation of \dot{Q} is a true representation of \dot{Q} . The only two derivatives which are not influenced by the assumption of constant parameters are $\dot{\rho}_Q$ and \dot{J}_T . The aim of an observer can be formulated as

$$\min_x \|y - h(x)\|_2$$

where x is the state vector, y is the output measurement, and $h(x)$ is the measurement as given by the model. Although an x could possibly be found such that $\|y - h(x)\|_2 = 0$, this will not necessarily be the true system state because of the model uncertainty and mismatch between $h(x)$ and y .

As mentioned in Section 1, the model considered here is reduced in Le Roux et al. (2016b) such that the states and parameters are linearly observable from the measurements J_T , Q , ρ_Q , and $\dot{\rho}_Q$. The success of the filter can be attributed to the fact that the representations of the measurements in terms of the modelled states are not dependent on the assumption of constant parameters, and are therefore relatively accurate symbolic representations of the measurements. However, this comes at the cost of distinguishing between x_r and x_b , as these two states are considered as one state x_{rb} in the reduced model.

Ideally a further measurement is desired which can assist with the estimation procedure. As mentioned previously, a model of the power draw of the mill can be used to estimate x_b (Apelt et al., 2001). The difficulty with using the power draw model is that it introduces further parameters to estimate, which increases the complexity of the state and parameter estimation task.

$$\begin{bmatrix} J_T \\ Q \\ \rho_Q \\ \dot{J}_T \\ \dot{Q} \\ \dot{\rho}_Q \\ \ddot{J}_T \\ \ddot{Q} \\ \ddot{\rho}_Q \end{bmatrix} = \begin{bmatrix} X_{ws} + x_r + x_b \\ v_{mill} \\ \eta(x_w + x_s)^2 \\ \frac{(\rho_w x_w + \rho_o x_s)}{(x_w + x_s)} \\ -\eta X_{ws}^2 - V_{bi} - V_{ri} - V_{si} - V_{wi} + x_b K_b \\ -2\eta^2 X_{ws}^3 + 2\eta K_r x_r X_{ws} + 2\eta X_{ws} V_{ws} \\ \frac{(\rho_o - \rho_w)(x_w x_r K_r + V_{si} x_w - V_{wi} x_s)}{X_{ws}^2} \\ 2\eta^2 X_{ws}^3 - 2\eta K_r x_r X_{ws} - 2\eta X_{ws} (V_{si} + V_{wi}) - V_{bi} K_b + x_b K_b^2 \\ 6\eta^3 X_{ws}^4 - 8\eta^2 X_{ws}^2 (K_r x_r + V_{ws}) + 2\eta K_r^2 x_r (x_r - X_{ws}) + 2\eta K_r V_{ri} X_{ws} + 4\eta K_r x_r V_{ws} + 2\eta V_{ws}^2 \\ (\rho_o - \rho_w) \left(x_r K_r x_w (\eta X_{ws}^2 - 2x_r K_r - K_r X_{ws}) + \eta (V_{si} x_w X_{ws}^2 - V_{wi} x_s X_{ws}^2) - 2V_{si}^2 x_w + 2V_{wi}^2 x_s \right) \\ X_{ws}^3 \end{bmatrix} \quad (11)$$

4. CONCLUSION

The model of Le Roux et al. (2016c) represents the constituents of a mill using four states: water, solids, rocks and balls. The grinding environment is modelled using the following constant parameters: a discharge rate, an abrasion rate for rocks, and an abrasion rate for balls. Although all states and parameters are locally (weakly) nonlinear observable from the measurements of the mill filling, discharge flow-rate and discharge density, the states and parameters are not observable from the linearised system. The system can be reduced such that all states and parameters are observable from the linearised version of the reduced model, but this comes at the cost of lumping rocks and balls together (Le Roux et al., 2016b).

This study aims to indicate what measurements are required to distinguish between the rocks and balls in the mill. As seen from the observability analysis, the states and parameters for the full model presented in Section 2.2 become nonlinearly observable from the second order derivatives of the measurements. If the model is extended to include these second order derivatives in the measurement vector, all states and parameters are observable from the linearised version of this extended model.

Of the three available measurements, the mill filling and the discharge density are most valuable for gaining insight into conditions inside the mill. The time-derivatives of the discharge density is required for successful estimation of all mill states, and consequently to successfully distinguish between rocks and balls. The first-order time-derivative of the discharge density can be represented fairly accurately by the model states. However, modelling the second-order derivative of the discharge density proves problematic, as the symbolic expression of the derivative is dependent on the assumption of constant model parameters.

Given the information regarding mill constituents which can be obtained from measuring the mill discharge density, this works aims to motivate the inclusion of measurement instrumentation at the mill discharge. This would require careful consideration of mill discharge trommel design to allow sufficient space to install the required instrumentation. Although the combined volume of rocks and balls can be estimated using mill filling, discharge flow-rate, and discharge density measurements, these measurements remain insufficient to distinguish between rocks and balls. For future work, an additional, viable, and independent measurement is required to reliably estimate and distinguish between the volume of balls and rocks in the mill.

REFERENCES

- Apelt, T.A., Asprey, S.P., and Thornhill, N.F. (2001). Inferential measurement of SAG mill parameters. *Minerals Eng.*, 14(6), 575–591.
- Apelt, T.A., Asprey, S.P., and Thornhill, N.F. (2002). Inferential measurement of SAG mill parameters II: State estimation. *Minerals Eng.*, 15, 1043–1053.
- Herbst, J.A. and Pate, W.T. (1999). Object components for comminution system softsensor design. *Powder Tech.*, 105, 424–429.
- Herbst, J.A., Pate, W.T., and Oblad, A.E. (1992). Model-based control of mineral processing operations. *Powder Tech.*, 69, 21–23.
- Herbst, J.S. and Pate, W.T. (1996). On-line estimation of charge volumes in semi-autogenous and autogenous grinding mills. In *Proc. SAG 1996, Vancouver, B.C., Canada*, 817–827.
- Herbst, J.S., Pate, W.T., and Oblad, A.E. (1989). Experiences in the use of model-based expert control systems in autogenous and semi-autogenous grinding circuits. In *Proc. SAG 1989, Vancouver, B.C., Canada*, 669–686.
- Hermann, R. and Krener, A.J. (1977). Nonlinear controllability and observability. *IEEE Trans. Automatic Control*, AC-22(5), 728–740.
- Hinde, A.L. and Kalala, J.T. (2009). The application of a simplified approach to modelling tumbling mills, stirred media mills and HPGR's. *Minerals Eng.*, 22(7-8), 633–641.
- Latchireddi, S. and Morrell, S. (2003). Slurry flow in mills: grate-only discharge mechanism (Part-1). *Minerals Eng.*, 16, 625–633.
- Le Roux, J.D. and Craig, I.K. (2016). State and parameter identifiability of a nonlinear grinding mill circuit model. In *Proc. 17th IFAC Symposium Mining Mineral Metal Processing*. Vienna, Austria.
- Le Roux, J.D., Olivier, L.E., Naidoo, M.A., Padhi, R., and Craig, I.K. (2016a). Throughput and product quality control for a grinding mill circuit using non-linear MPC. *J. Process Control*, 42, 35–50.
- Le Roux, J.D., Steinboeck, A., Kugi, A., and Craig, I.K. (2016b). An EKF observer to estimate semi-autogenous grinding mill hold-ups. *J. Process Control*. Submitted for Review.
- Le Roux, J.D., Steinboeck, A., Kugi, A., and Craig, I.K. (2016c). Nonlinear observability of grinding mill conditions. In *Proc. 17th IFAC Symposium Mining Mineral Metal Processing*. Vienna, Austria.
- Morrell, S. and Stephenson, I. (1996). Slurry discharge capacity of autogenous and semi-autogenous mills and the effect of grate design. *Int. J. Mineral Process.*, 46, 53–72.
- Napier-Munn, T.J., Morrell, S., Morrison, R.D., and Kojovic, T. (2005). *Mineral Comminution Circuits: Their Operation and Optimisation*. JKMRRC Monograph Series in Mining and Mineral Processing, Isles Road, Indooroopilly, Queensland 4068, Australia, 3rd edition.
- Olivier, L.E., Huang, B., and Craig, I.K. (2012). Dual particle filters for state and parameter estimation with application to a run-of-mine ore mill. *J. Process Control*, 22(4), 710–717.
- Powell, M.S., Perkins, T., and Mainza, A.N. (2011). Grind-curves applied to a range of SAG and AG mills. In *Proc. SAG 2011, Vancouver, B.C., Canada*.
- Powell, M.S., van der Westhuizen, A.P., and Mainza, A.N. (2009). Applying grindcurves to mill operation and optimisation. *Minerals Eng.*, 22(7-8), 625–632.
- Savitzky, A. and Golay, M.J.E. (1964). Smoothing and differentiation of data by simplified least squares procedures. *Analytical Chemistry*, 36(8), 1627–1629.
- Wei, D. and Craig, I.K. (2009). Grinding mill circuits - A survey of control and economic concerns. *Int. J. Mineral Process.*, 90(1-4), 56 – 66.